# The coding genome of splenic marginal zone lymphoma: activation of *NOTCH2* and other pathways regulating marginal zone development

Davide Rossi,[1] Vladimir Trifonov,[2] Marco Fangazio,[1,3] Alessio Bruscaggin,[1] Silvia Rasi,[1] Valeria Spina,[1] Sara Monti,[1] Tiziana Vaisitti,[4] Francesca Arruga,[4] Rosella Famà,[1] Carmela Ciardullo,[1] Mariangela Greco,[1] Stefania Cresta,[1] Daniela Piranda,[1] Antony Holmes,[3] Giulia Fabbri,[3] Monica Messina,[3] Andrea Rinaldi,[5] Jiguang Wang,[2] Claudio Agostinelli,[6] Pier Paolo Piccaluga,[6] Marco Lucioni,[7] Fabrizio Tabbò,[8] Roberto Serra,[9] Silvia Franceschetti,[1] Clara Deambrogi,[1] Giulia Daniele,[10] Valter Gattei,[11] Roberto Marasca,[12] Fabio Facchetti,[13] Luca Arcaini,[14] Giorgio Inghirami,[8] Francesco Bertoni,[5] Stefano A. Pileri,[6] Silvia Deaglio,[4] Robin Foà,[15] Riccardo Dalla-Favera,[3,16,17] Laura Pasqualucci,[3,16,18] Raul Rabadan,[2] and Gianluca Gaidano[1]

[1]Division of Hematology and [9]Laboratory of Medical Informatics, Department of Translational Medicine, Amedeo Avogadro University of Eastern Piedmont, 28100 Novara, Italy
[2]Department of Biomedical Informatics and Center for Computational Biology and Bioinformatics, [3]Institute for Cancer Genetics and the Herbert Irving Comprehensive Cancer Center, [16]Department of Pathology and Cell Biology, and [17]Department of Genetics and Development, Columbia University, New York, NY 10032
[4]Department of Genetics, Biology and Biochemistry and Human Genetics Foundation, and [8]Department of Pathology, Center for Experimental Research and Medical Studies (CeRMS), University of Turin, 10126 Turin, Italy
[5]Institute of Oncology Research and Oncology Institute of Southern Switzerland, CH-6500 Bellinzona, Switzerland
[6]Haematopathology, Department L. and A. Seragnoli, University of Bologna, 40138 Bologna, Italy
[7]Division of Pathology and [14]Division of Hematology, Fondazione IRCCS Policlinico San Matteo, University of Pavia, 27100 Pavia, Italy
[10]Hematology Unit, National Cancer Center of Bari and Department of Biology, University of Bari, 70126 Bari, Italy
[11]Clinical and Experimental Onco-Hematology, CRO, IRCCS, 33081 Aviano, Italy
[12]Division of Hematology, University of Modena and Reggio Emilia, 41124 Modena, Italy
[13]Division of Pathology, Spedali Civili, University of Brescia, 26123 Brescia, Italy
[15]Division of Hematology, Department of Cellular Biotechnologies and Hematology, Sapienza University, 00618 Rome, Italy
[18]Institute of Hematology, University of Perugia, 06132 Perugia, Italy.

**Splenic marginal zone lymphoma (SMZL) is a B cell malignancy of unknown pathogenesis, and thus an orphan of targeted therapies. By integrating whole-exome sequencing and copy-number analysis, we show that the SMZL exome carries at least 30 nonsilent gene alterations. Mutations in *NOTCH2*, a gene required for marginal-zone (MZ) B cell development, represent the most frequent lesion in SMZL, accounting for ~20% of cases. All *NOTCH2* mutations are predicted to cause impaired degradation of the NOTCH2 protein by eliminating the C-terminal PEST domain, which is required for proteasomal recruitment. Among indolent B cell lymphoproliferative disorders, *NOTCH2* mutations are restricted to SMZL, thus representing a potential diagnostic marker for this lymphoma type. In addition to *NOTCH2*, other modulators or members of the NOTCH pathway are recurrently targeted by genetic lesions in SMZL; these include *NOTCH1*, *SPEN*, and *DTX1*. We also noted mutations in other signaling pathways normally involved in MZ B cell development, suggesting that deregulation of MZ B cell development pathways plays a role in the pathogenesis of ~60% SMZL. These findings have direct implications for the treatment of SMZL patients, given the availability of drugs that can target NOTCH, NF-κB, and other pathways deregulated in this disease.**

CORRESPONDENCE
Riccardo Dalla-Favera:
rd10@columbia.edu
OR
Gianluca Gaidano:
gaidano@med.unipmn.it

Abbreviations used: DLBCL, diffuse large B cell lymphoma; HCV, hepatitis C virus; IGHV, immunoglobulin heavy chain variable; MZ, marginal zone; OS, overall survival; PFS, progression-free survival; SMZL, splenic marginal zone lymphoma; SNP, single nucleotide polymorphism.

D. Rossi, V. Trifonov, and M. Fangazio contributed equally to this paper.
R. Dalla-Favera, L. Pasqualucci, R. Rabadan, and G. Gaidano contributed equally to this paper.



Supplemental material can be found at:
http://doi.org/10.1084/jem.20120904

The Rockefeller University Press $30.00
J. Exp. Med. 2012 Vol. 209 No. 9 1537-1551
www.jem.org/cgi/doi/10.1084/jem.20120904

Splenic marginal zone (MZ) lymphoma (SMZL) is a neoplasm of mature B cells that affects elderly patients and involves the spleen, bone marrow, and peripheral blood, while typically sparing peripheral lymph nodes and other sites populated by MZ B cells, namely mucosa-associated lymphoid tissue sites (Matutes et al., 2008; Swerdlow et al., 2008; Traverse-Glehen et al., 2011). Within the spleen, tumor cells are represented by small lymphocytes that occupy the MZ surrounding germinal centers and infiltrate the red pulp (Swerdlow et al., 2008). Despite an indolent behavior in the majority of patients, ∼25% of SMZL patients experience a progressive course leading to early death (Matutes et al., 2008; Salido et al., 2010).

The pathogenesis of SMZL is currently elusive. Clinical and epidemiological data point to an association with hepatitis C virus (HCV); however, the infection rate in SMZL patients does not exceed ∼15%, even in geographic areas in which the virus is endemic (Hermine et al., 2002; Suarez et al., 2006). The contribution of antigen stimulation to SMZL pathogenesis is suggested by the highly restricted immunoglobulin gene repertoire, including selective usage of the immunoglobulin heavy chain variable (*IGHV*) *1-2*04* allele in ∼20–30% of cases, but the relevant antigen has not been identified (Warsame et al., 2011; Bikos et al., 2012).

Although the molecular pathogenesis of many lymphoma entities has been elucidated in detail (Swerdlow et al., 2008), relatively little is known about the genetic lesions associated with SMZL. Deletions of 7q31-q32 and gains of 3q are recurrent in ∼20–30% and ∼10–20% of cases, respectively, but the genes targeted by these lesions are unknown (Salido et al., 2010; Watkins et al., 2010; Rinaldi et al., 2011; Robledo et al., 2011). Cancer genes known to harbor genetic lesions in SMZL are not specific for this lymphoma type, and are limited to *TP53*, which is disrupted in ∼15% of cases, most likely as a secondary genetic alteration (Gruszka-Westwood et al., 2001; Salido et al., 2010; Rinaldi et al., 2011), and to genes of the NF-κB pathway, which are mutated in ∼30% of cases (Rossi et al., 2011; Yan et al., 2012). Scant knowledge of somatic gene lesions associated with SMZL limits the present understanding of its pathogenesis and hampers the possibility of diagnosis and classification based on genetics, one of the mainstay criteria adopted by the World Health Organization Classification of Tumours of Hematopoietic and Lymphoid Tissues for the diagnosis of B cell lymphoma (Swerdlow et al., 2008).

By integrating whole-exome sequencing and genome-wide high-density single nucleotide polymorphism (SNP) array data, this study identifies alterations of key regulators of MZ development in ∼60% of SMZL patients, with *NOTCH2* representing the most frequently mutated gene in this lymphoma type.

## RESULTS

### Identification of recurrent targets of genetic alterations in SMZL

To discover somatic, nonsilent mutations and copy number aberrations (CNAs) that are clonally represented in the SMZL coding genome, and presumably contributed to the initial expansion of the tumor clone, we performed massively parallel sequencing and high-density SNP array analysis of paired tumor and normal DNA from eight untreated individuals diagnosed with SMZL (Table S1).

After enrichment of protein-coding genes by a hybridization-capture method, next-generation sequencing was performed using the Illumina HiSeq2000 instrument (Table S2). The whole-exome sequencing approach allowed us to map an average of ∼102.5 million reads per sample at a mean depth of 110.6× (range, 59.0-137.0× per sample), with an average of 83.3% of the target sequence being covered by at least 30 reads (range, 72.0–86.0%; Table S2). Bioinformatic analysis followed by Sanger resequencing validation confirmed the presence of 203 somatic, nonsilent mutations (mean, 25.3/case; range, 12–44/case), affecting 191 distinct genes (validation rate, 92.6%; Fig. 1, A–D, and Table S3). The relative expression of the variant allele was determined by transcriptome analysis, performed in 6 of the 8 cases (Table S3).

By using the Affymetrix SNP6.0 platform, 41 somatic CNAs (30 deletions and 11 gains) were identified in the 8 discovery SMZL cases (mean, 5.1/case; range, 0–19/case; Fig. 1 E and Table S4). Alterations known to be associated with SMZL (3q gain, 7q31-q32 deletion, 17p deletion) and previously detected by FISH were correctly identified using the SNP array approach. Of the 41 CNAs, 8 (7 losses and 1 gain) were defined as focal, i.e., spanning ≤3 genes, with none being recurrently observed. When combining point mutations and CNAs, the overall load of tumor-acquired lesions was heterogeneous across the 8 SMZL cases investigated, ranging from 13–60 lesions/case (mean load, 30.5 lesions/case; Fig. 1 F).

Genes identified through the whole-exome sequencing and high-resolution SNP array approaches were prioritized for further assessment of their mutation frequency according to the fulfillment of one or more of the following criteria: (a) mutation recurrence in the discovery panel; (b) involvement by both point mutations and focal copy number changes or truncating deletions; and (c) involvement in cellular pathways known a priori to be potentially relevant for SMZL biology. The analysis was also extended to selected genes that were either involved in the same pathways as the genes found to be altered in the discovery genomes ($n = 7$, including *NOTCH1*, *FBXW7*, *SPEN*, *PTEN*, *CTNNB1*, *CD79A*, and *CD79B*) and/or those previously implicated in SMZL pathogenesis ($n = 7$, including *IKBKB*, *TNFAIP3*, *TRAF3*, *MAP3K14*, *TP53*, *CARD11*, and *MYD88*; Rossi et al., 2011; Yan et al., 2012), even if they were not identified in the discovery phase. Based on these criteria, 61 genes (47 revealed by the genomic approach in the discovery panel, and 14 involved in the same pathways as genes mutated in the discovery genome) were analyzed by Sanger-based resequencing of their coding exons and consensus splice sites in an independent screening panel of 32 SMZL cases (Table S5); for selected genes, an additional extension panel of 77 SMZL cases was also analyzed (Table S6; total number of cases, 109).

Of the 61 genes investigated, 21 were found to be mutated in at least two SMZL cases, and 18 were altered in ≥5%

of cases. Overall, the genes that are recurrently mutated in SMZL point to the involvement of specific programs implicated in normal MZ development (NOTCH, NF-κB, B cell receptor, and Toll-like receptor signaling), as well as in chromatin remodeling and transcriptional regulation.

### Alterations of *NOTCH2*

A molecular feature of SMZL revealed by this study is the presence of recurrent lesions in genes encoding for components of the NOTCH signaling pathway, a master regulator of normal MZ development (Kuroda et al., 2003; Saito et al., 2003;

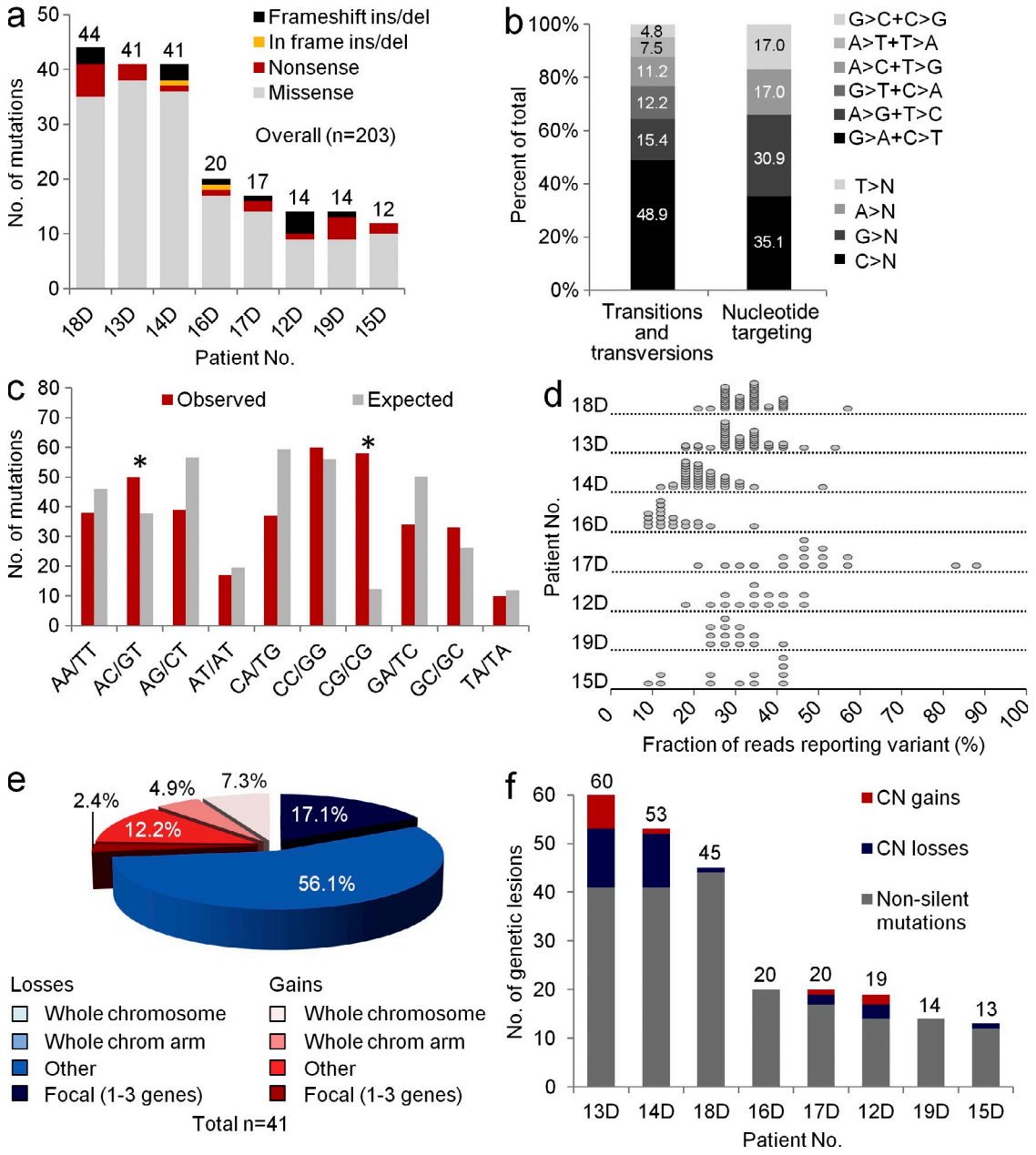


**Figure 1. SMZL coding genome complexity.** (a) Number and type of nonsilent mutations identified in the 8 discovery genomes. (b) The pattern of nucleotide substitutions in the discovery genomes revealed a predominance of transitions over transversions (121:67, ratio of 1.8) and a preferential targeting of G and C nucleotides (66.0% affecting G/C compared with 34.0% affecting A/T nucleotides). (c) Mutation frequency at specific dinucleotides (red bars). A significant bias toward alterations at 5′-CpG-3′ dinucleotides, which accounted for 15.4% of all missense and nonsense changes, was documented. The expected frequencies (gray bars) correspond to the dinucleotide sequence composition of the Consensus CDS. Asterisks denote statistically significant differences in overrepresented changes, as assessed by a Poisson distribution after correction for multiple hypotheses. (d) Fraction of sequencing reads reporting individual somatic nonsilent variants (gray circles) in the discovery genomes. The large majority of the nonsilent mutations (82.1%) were present in at least 20% of the reads. (e) Overall number and frequency of somatically acquired CNAs. Losses of whole chromosomal arms were not observed and are thus not reported in the figure. (f) Combined load of somatically acquired genetic lesions in the discovery genomes, including nonsilent mutations and CNAs.

Moran et al., 2007; Santos et al., 2007; Pillai and Cariappa, 2009; Hampel et al., 2011). Targeted resequencing of *NOTCH2*, a gene required for MZ B cell differentiation (Saito et al., 2003; Moran et al., 2007; Pillai and Cariappa, 2009; Hampel et al., 2011), showed recurrent mutations in 25/117 (21.3%) SMZLs, including 2/8 (25.0%) discovery cases and 23/109 (21.1%) cases from the screening/extension panels. These data establish *NOTCH2* as the most frequently mutated gene in SMZL (Fig. 2).

*NOTCH2* mutations were represented in all instances by truncating events (14 frameshift indels and 11 nonsense mutations), and clustered within a hotspot region in exon 34, including a recurrent p.R2400* nonsense mutation in 6/25 (24.0%) cases (Fig. 3 A, Tables S3, and Table S7). *NOTCH2* mutations were consistently absent in the heterodimerization domain or in other portions of the gene that are targeted by inactivating mutations in different cancer types (Wang et al., 2011b). Based on their distribution, all mutations were predicted to cause impaired degradation of the NOTCH2 protein through the elimination or truncation of the C-terminal PEST domain (Fig. 3 A). Analysis of paired normal DNA confirmed the somatic origin of the mutations in all cases for which material was available ($n$ = 13). *NOTCH2* mutations were present in ~40% of the reads by transcriptome sequencing, indicating allelic balance in the expression of the WT and mutated allele (Table S3). Western blot analysis of NOTCH2 expression consitently revealed the presence of an aberrant band of lower molecular weight, corresponding in size to the predicted truncated NOTCH2 protein, in all mutated cases studied (Fig. 4). Copy number gains of *NOTCH2* were never observed in 110 SMZL cases analyzed by SNP array and/or FISH analysis.

In 3 patients for which multiple samples were available from different involved organs, the same *NOTCH2* mutation was detectable at all sites, namely peripheral blood, bone marrow, and spleen. This observation suggests that the mutation had been acquired before dissemination of the lymphoma clone to multiple anatomical sites.

To verify the specificity of *NOTCH2* mutations for SMZL, *NOTCH2* was investigated across the clinico-pathological spectrum of mature B cell tumors ($n$ = 399). *NOTCH2* mutations were consistently absent in nodal MZ lymphoma (0/18), chronic lymphocytic leukemia (0/100), mantle cell lymphoma (0/20), follicular lymphoma (0/20), hairy cell leukemia (0/20), and multiple myeloma (0/22), whereas they occurred sporadically in extranodal MZ lymphoma (1/65, 1.5%) and, in accordance with a previous study (Lee et al., 2009), were restricted to 5/134 (3.7%) diffuse large B cell lymphomas (DLBCL; Fig. 3 B).

The clinical impact of *NOTCH2* mutations on SMZL overall survival (OS) was assessed in 94 patients with available

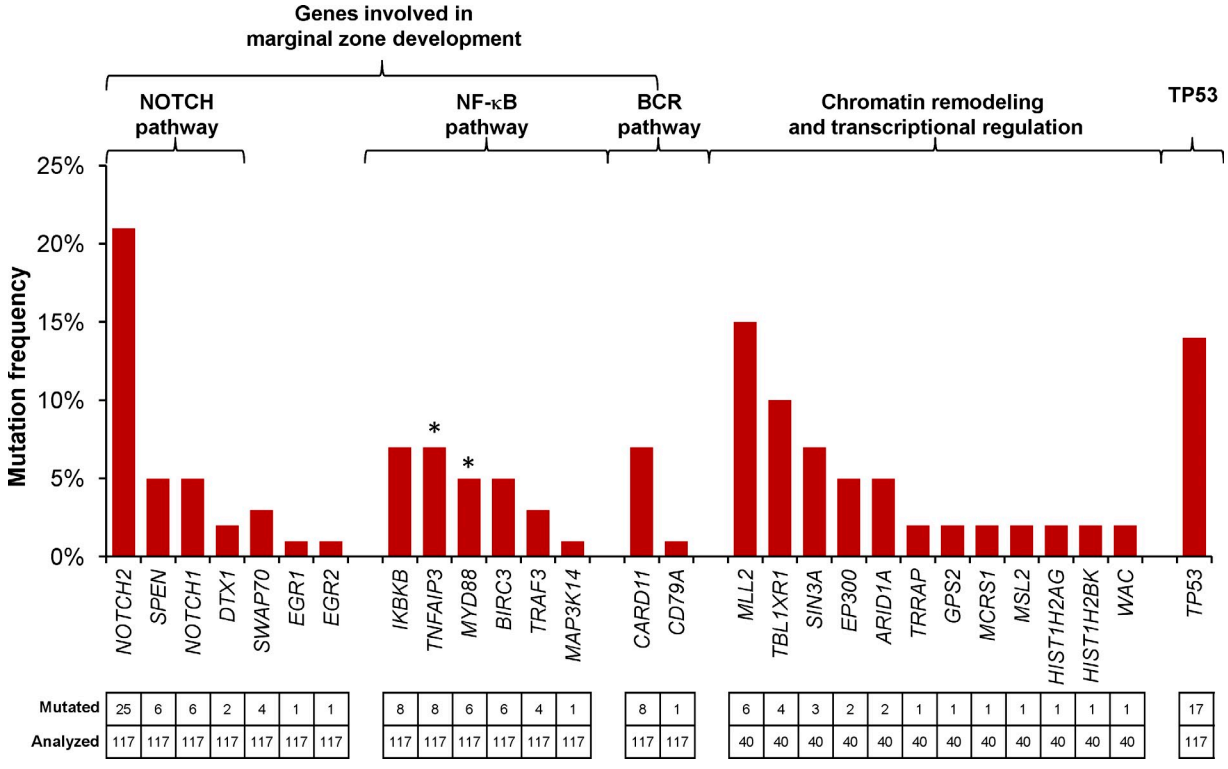


**Figure 2. Recurrently targeted pathways in SMZL.** Percentage of SMZL cases harboring mutations in selected genes belonging to cellular pathways that are recurrently altered in SMZL. Numbers at the bottom indicate the actual number of mutated cases over the total samples analyzed. Asterisks denote genes that are also implicated in Toll-like receptor responses. BCR, B cell receptor.

follow up. Consistent with the indolent behavior of this lymphoma type, the 5-yr OS of the SMZL cohort was 78.1% (95% CI, 67.8–88.4%). At 5 yr, SMZL patients harboring *NOTCH2* mutations were characterized by a significantly higher OS probability (93.3%; 95% CI, 80.0–100%) compared with patients harboring a WT *NOTCH2* (74.3%; 95% CI, 61.4–87.2%; P = 0.048; Fig. 5). Consistent with the improved OS, cases harboring *NOTCH2* mutations displayed a longer progression-free survival (PFS) after first-line treatment compared with *NOTCH2* WT patients (5-yr PFS in *NOTCH2* mutated patients, 83%; 95% CI, 65.4–100%; 5-yr PFS in *NOTCH2* WT patients, 44.1%; 95% CI, 28.9–58.3%; P = 0.020). There were no differences in major adverse events between *NOTCH2*-mutated and unmutated patients, as documented by a similar treatment-related mortality in the two groups (*NOTCH2*-mutated patients, 0/18; *NOTCH2* WT patients 1/53, 1.8%; P = 1.000).

Overall, these data document that, among B cell neoplasia, *NOTCH2*-activating mutations are predominantly associated with SMZL, and underscore the genetic individuality of SMZL versus other MZ-derived lymphomas and versus indolent B cell lymphoproliferative disorders clinically mimicking SMZL.

### Alterations in other genes of the NOTCH pathway

In addition to *NOTCH2*, other genes involved in NOTCH signaling and known to be relevant for normal MZ differentiation were affected by genomic lesions in SMZL, including *NOTCH1*, *SPEN*, and *DTX1* (Fig. 2; Kuroda et al., 2003; Saito et al., 2003; Santos et al., 2007; Pillai and Cariappa, 2009).

*NOTCH1*, a paralogue of *NOTCH2* implicated in several phases of lymphoid development, including terminal B cell differentiation into immunoglobulin-secreting cells (Santos et al., 2007; Yuan et al., 2010), was affected in 6/117 (5.1%) SMZLs by a recurrent 2-bp deletion (p.P2515fs*4) that truncates the PEST domain, similar to *NOTCH2* lesions (Fig. 6 A and Table S7). This deletion also represents the most common *NOTCH1* alteration in chronic lymphocytic leukemia and mantle cell lymphoma (Fabbri et al., 2011; Wang et al., 2011a; Kridel et al., 2012;

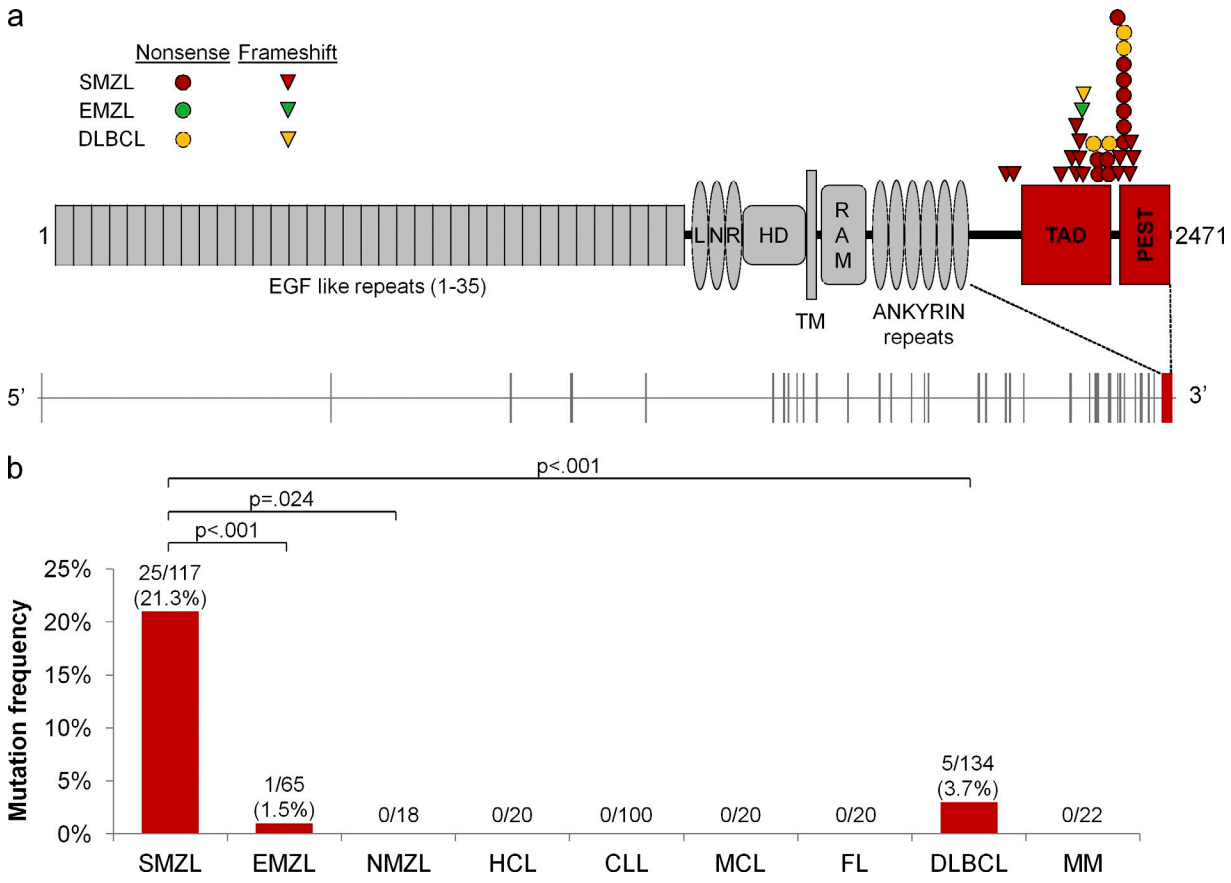


**Figure 3.** ***NOTCH2* is frequently mutated in SMZL.** (a) Schematic representation of the human NOTCH2 gene (bottom) and protein (top), with its key functional domains (EGF, epithelial growth factor; LNR, LIN-12/NOTCH repeats; HD, heterodimerization; TM, transmembrane; RAM, regulation of amino acid metabolism; TAD, transactivation domain). Color-coded symbols indicate the type and position of the mutations. (b) Prevalence of *NOTCH2* mutations among mature B cell tumors (EMZL, extranodal MZ lymphoma; NMZL, nodal MZ lymphoma; HCL, hairy cell leukemia; CLL, chronic lymphocytic leukemia; MCL, mantle cell lymphoma; FL, follicular lymphoma; MM, multiple myeloma). Numbers on the top indicate the actual number of mutated cases over the total samples analyzed.

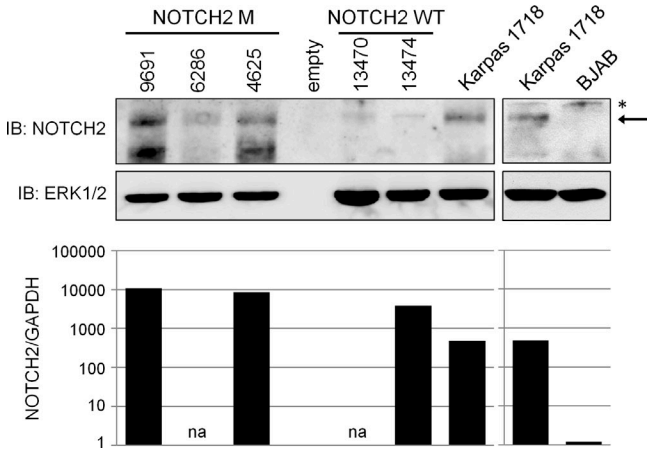


**Figure 4. NOTCH2 expression in SMZL.** Western blot analysis of NOTCH2 protein expression in purified primary tumor cells from 5 SMZL cases carrying WT or mutated (M) *NOTCH2*, and in the SMZL cell line Karpas 1718, also WT for *NOTCH2* (left); the specificity of the antibody was validated by using the BJAB cell line, which lacks *NOTCH2* mRNA expression (right; asterisk indicates nonspecific band). Arrow indicates the intact NOTCH2 protein; a band of lower molecular weight, consistent with the predicted size of the NOTCH2 protein encoded by the mutant allele, can be detected in all *NOTCH2*-mutated patients, but not in *NOTCH2* WT samples. Where available, the relative *NOTCH2* mRNA levels in the same samples are quantified by qRT-PCR (bottom; na, not available).

Quesada et al., 2012; Rossi et al., 2012), and the most recurrent *NOTCH1* PEST domain mutation in T cell acute lymphoblastic leukemia, where it causes impaired degradation of the NOTCH1 protein (Weng et al., 2004).

*SPEN*, also known as *MINT*, has been reported to repress NOTCH signaling by physically interacting with and causing inhibition of the transcription factor RBPJ, which is implicated in the NOTCH signaling cascade (Kuroda et al., 2003; Li et al., 2005; VanderWielen et al., 2011). Consistent with its biochemical function, *SPEN* physiologically acts in the immune system as a negative regulator of B lymphocyte differentiation into MZ B cells by counteracting NOTCH activation (Kuroda et al., 2003). *SPEN* was found to be mutated in 6/117 (5.1%) SMZL cases (Fig. 2). With one exception, *SPEN* mutations were represented by inactivating events, including three frameshift indels and two nonsense substitutions (Fig. 6 A and Table S7), which were documented to be of somatic origin in all cases with available paired normal DNA. *SPEN*-mutated alleles were predicted to encode truncated proteins lacking the C-terminal domain involved in the interaction of SPEN with RBPJ, and to be necessary for NOTCH signaling inhibition (Fig. 6 A; Kuroda et al., 2003). In addition to truncating mutations, *SPEN* was affected by one somatic missense substitution, categorized as probably damaging by PolyPhen-2 (Fig. 6 A and Table S7), and by four monoallelic deletions (Table S8). In all evaluable cases, *SPEN* mutations were restricted to a single allele and were not accompanied by deletions of the second allele. This pattern of predominant monoallelic inactivation is in agreement with in vitro models, suggesting that *SPEN* mutants may exert a dominant-negative effect (Li et al., 2005).

*DTX1* encodes a RING finger ubiquitin ligase that binds the NOTCH family proteins and modulates their signaling, is highly expressed in MZ B cells, and may be important for late steps of B cell differentiation (Izon et al., 2002; Saito et al., 2003). In 2/117 (1.7%) SMZLs, *DTX1* was affected by somatically acquired missense substitutions mapping within two functionally relevant domains: the WWE1 domain, which mediates physical interactions between DTX1 and NOTCH (Zweifel et al., 2005), and the proline-rich domain, which may serve as a docking site for NOTCH inhibitory factors (Matsuno et al., 2002; Fig. 6 A; Tables S3 and S7).

In summary, ∼32% (37/117) of SMZL patients carry alterations of genes belonging to the NOTCH pathway, with *NOTCH2* mutations accounting for approximately 2/3 of the events (25/37; 67.5%; Fig. 7).

## Alteration of additional pathways involved in MZ development

Besides NOTCH signaling, the development of a normal MZ requires B cell migration to and retention within the spleen marginal sinus until they are activated (Pillai and Cariappa, 2009). *SWAP70* encodes for an F-actin–binding/Rho GTPase–interacting protein that is necessary for

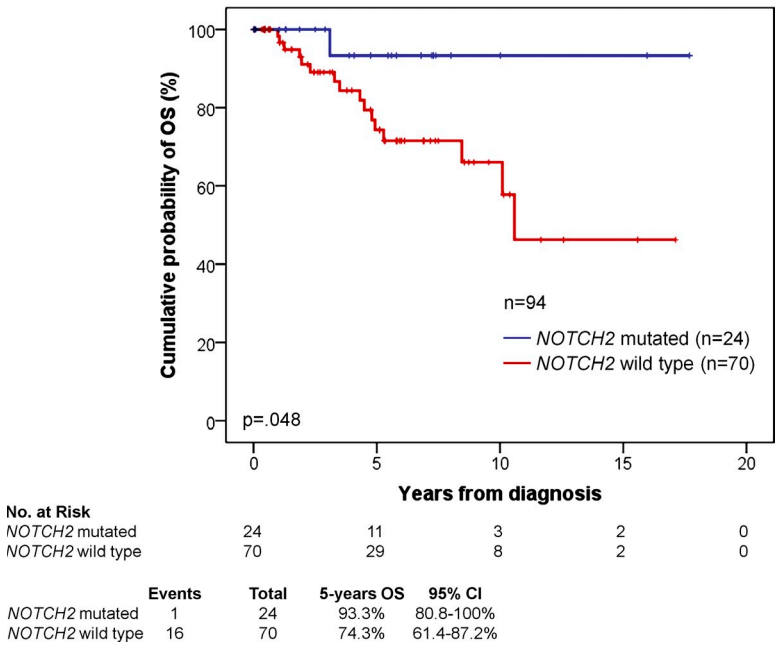


**Figure 5. *NOTCH2* mutations are associated with better OS.** Kaplan-Meier estimates of OS in SMZL patients ($n = 94$), according to *NOTCH2* mutation status.

normal B cell trafficking across spleen compartments (Chopin et al., 2010a, 2011). In 4/117 (3.4%) cases, *SWAP70* was disrupted by truncating mutations that removed the C-terminal domain of the protein required for binding to F-actin (Fig. 6 A; Tables S3 and S7). *SWAP70* was also affected by a monoallelic deletion in one additional SMZL (Table S4). Moreover, one SMZL (0.9%) displayed a somatic mutation in the *EGR1* B cell transcription factor, which also plays a role in MZ development (Table S3; Gururajan et al., 2008). *EGR2*, a paralogue of *EGR1*, was somatically mutated in one additional case (0.9%; Table S3).

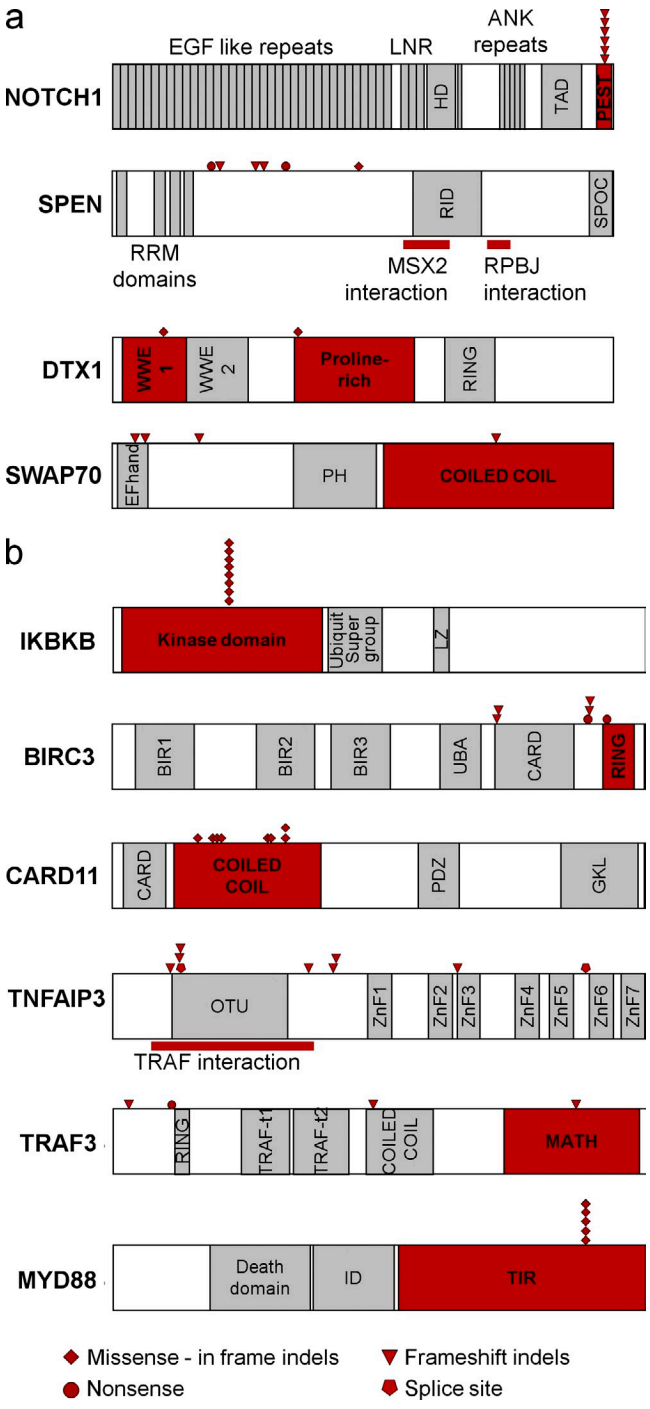


**Figure 6. Mutations of genes belonging to the NOTCH, migration/adhesion, NF-κB, and B cell receptor pathways in SMZL.** Schematic diagram of the proteins targeted by mutations in SMZL, with their key functional domains (a, NOTCH pathway; b, NF-κB pathway). Symbols indicate the type of mutation.

Active NF-κB signaling is necessary for the generation and/or maintenance of normal MZ B cells (Calado et al., 2010; Chu et al., 2011; Conze et al., 2010; Pappu and Lin, 2006; Moran et al., 2007; Xie et al., 2007; Sasaki et al., 2008; Pillai and Cariappa, 2009). Mutations of both the canonical (17/117, 14.5% cases) and noncanonical (11/117, 9.4% cases) NF-κB pathways were recurrent in SMZL (Fig. 2), and affected several previously identified genes in this lymphoma type (Rossi et al., 2011; Yan et al., 2012), including *IKBKB* (8/117, 6.8%), *TNFAIP3* (8/117, 6.8%), *BIRC3* (6/117, 5.1%), *TRAF3* (4/117, 3.4%), and *MAP3K14* (1/117, 0.9%; Fig. 6 B; Table S3 and Table S7). These genes were also targeted by CNAs, including deletions of *TNFAIP3* (8/110, 7.2%), *BIRC3* (7/110, 6.3%), and *TRAF3* (6/110, 5.4%), and gains of *MAP3K14* (7/110, 6.3%; Table S8).

In addition to genes specifically attributed to the NF-κB pathway, recurrent mutations were also found in *CARD11* and *MYD88*, which, among their many functions, act as positive regulators of NF-κB in signaling from the B cell receptor and Toll-like receptor, respectively (Fig. 2; Lenz et al., 2008; Ngo et al., 2011). *CARD11* mutations (6 missense and 2 in frame deletions) cluster within the coiled-coil domain in 8/117 (6.8%) cases (Fig. 6 B and Table S7). In 6/117 (5.1%) SMZLs, *MYD88* was targeted by a recurrent missense substitution (p.L265P) that has been previously reported in activated B cell–type DLBCL (Fig. 6 B and Table S7; Ngo et al., 2011).

Cases harboring NF-κB pathway mutations and cases harboring NOTCH pathway mutations did not differ in terms of clinical and biological features at presentation, including age, sex, performance status, levels of hemoglobin, LDH, β-2-microglobulin and albumin, HCV infection, *IGHV* mutation status, usage of the *IGHV1-2*04* allele, stereotyped VH CDR3, 7q31-q32 deletion, 3q gain, or *TP53* disruption ($P > 0.05$ in all instances).

Overall, mutations of positive and negative NF-κB regulators accounted for 40/117 (34.1%) SMZL cases (Fig. 7), implicating activation of NF-κB as a major contributor to the pathogenesis of this disease.

### Alteration of genes involved in chromatin remodeling and transcriptional regulation

Apart from genes implicated in MZ development, whole-exome sequencing revealed a second set of genes recurrently mutated in SMZL and regulating chromatin remodeling (Fig. 2). The *MLL2* histone methyltransferase controls gene transcription by modifying the lysine-4 position of histone 3 and is recurrently mutated in FL and DLBCL (Morin et al., 2011; Pasqualucci et al., 2011b). Inactivating mutations of

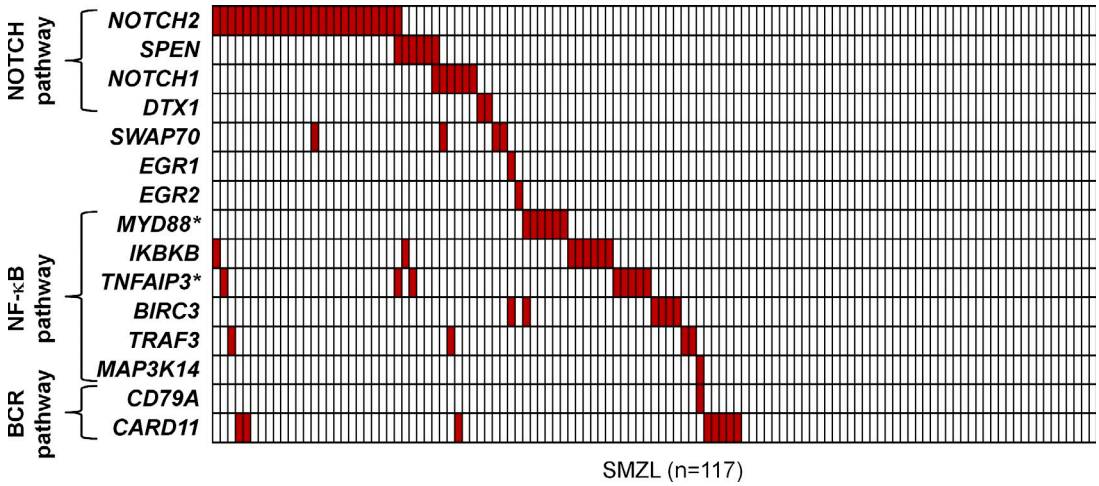


**Figure 7. Mutually exclusive involvement of genes implicated in MZ development.** In the heatmap, rows correspond to genes and columns represent individual patients. Color coding is based on gene mutation status (white, WT; red, mutated). Asterisks denote genes that also modulate Toll-like receptor responses. BCR, B cell receptor.

*MLL2* occurred in 6/40 (15.0%) SMZLs (Fig. 8; Tables S3 and S7), leading to removal or truncation of the C-terminal SET domain required for its enzymatic activity. In addition, two SMZLs showed a p.P692T somatic missense substitution. *ARID1A*, a member of the SWI-SNF chromatin remodeling family that was reported as mutated in several solid tumors (Wiegand et al., 2010), was targeted by genetic lesions in 4/40 (10.0%) cases, including 2 point mutations and 2 deletions (Fig. 8; Tables S3, S7 and S8). *EP300* and *CREBBP* are two highly related acetyltransferases that are also recurrently disrupted in B cell lymphoma (Pasqualucci et al., 2011a) and acute lymphoblastic leukemia (Mullighan et al., 2011). Somatic missense mutations of *EP300* were found in 2/40 (5%) SMZL cases (Fig. 8 and Table S3), whereas one additional patient harbored a small deletion that juxtaposes in-frame the first 16 exons of *CREBBP* to the C-terminal portion of the *ZNF434* gene, thus abrogating the CREBBP acetyltransferase domain, as confirmed by transcriptome sequencing analysis (not depicted). Somatic mutations of *SIN3A*, encoding for a core component of the SIN3–HDAC1/2 histone deacetylase complex, occurred in 3/40 (7.5%) SMZLs, and, in two cases, targeted regions that are required for the recruitment of histone modification complexes (Fig. 8; Tables S3 and S7; Grzenda et al., 2009). Other genes involved in chromatin remodeling and found to be somatically mutated in single SMZL cases are represented in Fig. 2.

Mutations were also detected in other transcriptional regulators. *TBL1XR1*, an intrinsic component of the SMRT-N-CoR transcription co-repressor machinery that was recently found to be recurrently disrupted in B cell tumors (Perissi et al., 2008), showed mutations in 4/40 (10.0%) SMZLs (Fig. 2). Mutations (two frameshift deletions and three somatically acquired missense substitutions) targeted the protein WD domains implicated in the exchange of nuclear receptor co-repressors for co-activators (Fig. 8; Table S3 and Table S7; Oberoi et al., 2011). *TBL1XR1* mutations were monoallelic in three cases, whereas one case harbored a disrupting mutation coupled to a missense substitution (Table S7).

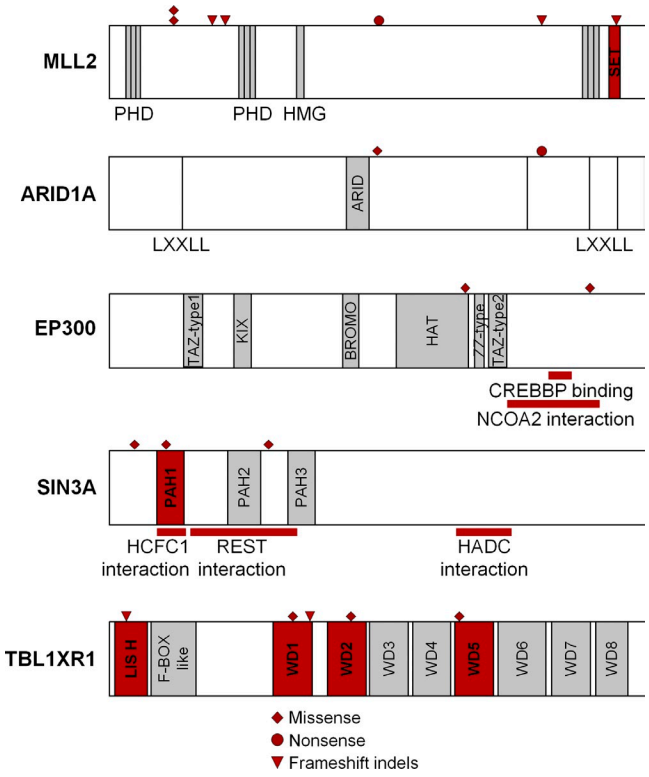


**Figure 8. Mutations of genes involved in chromatin remodeling and transcriptional regulation.** Schematic diagram of the indicated proteins, with their key functional domains. Symbols indicate the type of mutation.

Three additional SMZLs showed monoallelic *TBL1XR1* deletion (Table S8). *GPS2*, another member of the SMRT-N-CoR transcription co-repressor machinery that physically interacts with *TBL1XR1* (Oberoi et al., 2011), was biallelically inactivated in one SMZL by a nonsense mutation with deletion of the second allele (Table S3 and Table S4). The mutation targeted the *GPS2* domain required for *TBL1XR1* interaction. Monoallelic deletions of *GPS2* were observed in additional eight cases (Table S8).

Overall, mutations of chromatin remodeling and transcriptional regulation genes occurred in 14/40 (35.0%) SMZLs and, as observed in other cancer types (Gui et al., 2011), were frequently concurrent in the same patient (~50% of the mutations; Fig. 9), suggesting that they cooperate to promote tumorigenesis.

### Mutations of genes regulating MZ development and NF-κB activation characterize ~60% of SMZLs

Given the biological heterogeneity of SMZLs, we investigated the relationship between mutations of genes controlling MZ development and established genetic, immunogenetic, and biological subgroups of SMZLs, including those defined by deletion of 7q31-q32 (21/110, 19.1%), 3q gain (14/110, 12.7%), expression of unmutated *IGHV* genes (29/110, 26.3%), usage of the *IGHV1-2*04* allele (26/110, 23.6%), usage of stereotyped VH CDR3 (9/110, 8.1%), positive HCV serology (11/86, 12.7%), and *TP53* mutations (17/117, 14.5%). This analysis did not disclose any selective association, suggesting that mutations of genes controlling MZ development play an independent role in lymphomagenesis (Table S9). A preferential, though not selective, association was observed between deletion of 7q31-q32, a cytogenetic abnormality characteristic of SMZL, and cases harboring mutations of MZ development genes (19/64, 29.7% in cases harboring mutations vs. 2/46, 4.3% in cases devoid of mutations; $P = 0.001$; Table S9). In particular, deletion of 7q31-q32 significantly associated with SMZL harboring *NOTCH2* mutations (11/24, 45.8%; $P = 0.001$).

Mutations of genes implicated in MZ development (NOTCH, NF-κB, B cell receptor, and Toll-like receptor pathway, as well as *SWAP70*, *EGR1*, *EGR2*; Izon et al., 2002; Kuroda et al., 2003; Saito et al., 2003; Moran et al., 2007; Santos et al., 2007; Gururajan et al., 2008; Pillai and Cariappa, 2009; Chopin et al., 2010b, 2011; Hampel et al., 2011) show a largely mutually exclusive distribution pattern, although the number of cases ($n = 117$) lacks statistical power for this type of analysis (Fig. 7). Collectively, these lesions account for the majority of SMZL cases (70/117; 59.8%), and suggest that alterations in genes affecting B cell fate decision toward MZ differentiation represent alternative mechanisms converging on the deregulation of a common downstream target, which may include NF-κB.

## DISCUSSION

One goal of this study was to provide initial information on the landscape of somatic genetic lesions (type and frequency) that characterize the SMZL coding genome. Given the presence of ~25 nonsilent mutations and ~5 CNAs per case (on average, ~30 alterations/case), SMZL appears to show a degree of genomic complexity that is intermediate between that of aggressive lymphoma, namely DLBCL (~90 nonsilent mutations per case; Morin et al., 2011; Pasqualucci et al., 2011b; Lohr et al., 2012), and that of previously untreated chronic lymphocytic leukemia (~12 nonsilent mutations per case; Fabbri et al., 2011; Quesada et al., 2012), which shares an indolent course with SMZL.

A second key finding of this study was the identification of alterations in genes affecting B cell fate decision toward MZ differentiation as significantly associated with SMZL. Alterations in genes of the NOTCH pathway emerged as highly recurrent (~30%) in SMZL, with *NOTCH2*, a key regulator of MZ development, being the most frequently mutated gene (~20%). All *NOTCH2* mutations observed in SMZL cause disruption of the protein inhibitory PEST domain and are predicted to activate NOTCH2 signaling (Lee et al., 2009). Because of the lack of xenograft and cell line models of SMZL, we are currently unable to assess whether these mutations

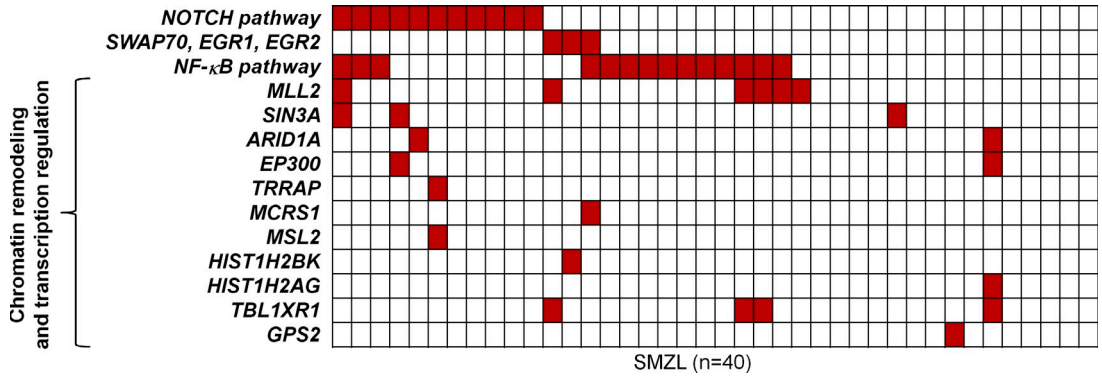


**Figure 9. Integrated analysis of mutations affecting chromatin remodeling genes in SMZL.** In the heatmaps, rows correspond to mutated genes and columns represent individual patients. Color coding is based on gene mutation status (white, WT; red, mutated). Analysis of chromatin remodeling genes was extended to the screening panel only (in total, 40 cases), and is thus shown separately.

confer ligand independence, or whether the mutated proteins still require activation by ligand binding. Disruption of the PEST domain renders SMZL-associated mutations of *NOTCH2* analogous to those involving *NOTCH1* in chronic lymphocytic leukemia and mantle cell lymphoma, and to a subset of *NOTCH1* mutations in T cell acute lymphoblastic leukemia (Fabbri et al., 2011; Wang et al., 2011a; Kridel et al., 2012; Quesada et al., 2012). Nevertheless, *NOTCH2* mutations appear to be relatively specific for SMZL, being virtually absent in other major types of mature B cell neoplasia and rare in DLBCL (Lee et al., 2009). Consistent with our findings, one single mutation of *NOTCH2* was recently described in one case of SMZL (Trøen et al., 2008). In addition to *NOTCH2*, other modulators or members of the NOTCH pathway were targeted by genetic lesions in SMZL, including *SPEN*, *DTX1*, and *NOTCH1*. The alternative involvement of multiple genes converging on the NOTCH pathway, together with the well-established functional role of some of these alterations, namely *NOTCH1* mutations in T cell acute lymphoblastic leukemia (Weng et al., 2004), strongly support their pathogenic role in SMZL.

As is the case for most cancer-associated genetic lesions, activation of *NOTCH2* may not be sufficient for malignant transformation. In fact, patients affected by the Hajdu-Cheney syndrome, an autosomal-dominant genetic disease that causes severe and progressive bone loss and is associated with germline *NOTCH2* mutations analogous to those identified in SMZL, do not develop lymphomas (Brennan and Pauli, 2001; Simpson et al., 2011). Similarly, transgenic mice engineered to express activating *NOTCH2* mutations in mature B cells display an expansion of the MZ at the expense of the follicular compartment, but do not develop lymphoma (Hampel et al., 2011). It is important to note, however, that lymphoma development may require longer times than those observed so far both in Hajdu-Cheney patients (no diagnosed individual was >50 yr old; Brennan and Pauli, 2001; Simpson et al., 2011) and in mice (1 yr), consistent with the elderly age and indolent course of SMZL (Hampel et al., 2011).

Collectively, the genetic alterations associated with SMZL appear to predominantly involve signaling pathways that regulate MZ development, including: (a) NOTCH, via the alternative mutation of multiple genes (*NOTCH2*, *NOTCH1*, *SPEN*, and *DTX1*); (b) NF-κB, via mutation of *TNFAIP/A20*, *BIRC3*, *TRAF3* and *CARD11*; and (c) the B cell receptor, via mutation of *CARD11*. Indeed, at least in mice, the commitment of mature B cells to the MZ compartment requires signaling from NOTCH2 (Kuroda et al., 2003; Saito et al., 2003; Moran et al., 2007; Santos et al., 2007; Pillai and Cariappa, 2009; Hampel et al., 2011), as well as activation of the NF-κB transcription complex (Xie et al., 2007; Sasaki et al., 2008; Calado et al., 2010; Conze et al., 2010; Chu et al., 2011) and possibly antigen stimulation through the B cell receptor and Toll-like receptor (Pappu and Lin, 2006). The alteration of genes implicated in the physical retention of MZ B cells within the spleen might also be important for SMZL pathogenesis, as suggested by the observation of recurrent mutations in *SWAP70* (Chopin et al., 2010a, 2011). Thus, the finding that ∼60% of SMZL cases display the alternative deregulation of these pathways suggests that one major component of SMZL pathogenesis is the constitutive activation of signals normally deputed to the differentiation and homing of B cells into the MZ.

Finally, the results herein have important implications for the clinical management of SMZL. Because the differential diagnosis of SMZL from other indolent B cell lymphoproliferative disorders clinically mimicking SMZL is often complex (Matutes et al., 2008; Swerdlow et al., 2008), some of the genetic alterations reported here, specifically mutations of *NOTCH2*, may serve as potentially helpful markers. More importantly, the results of this study provide a rationale for the design of novel therapeutic strategies for SMZL, which, to date, remains a disease orphan of specifically targeted drugs (Traverse-Glehen et al., 2011). New regimens may be useful to avoid splenectomy, a well-established therapeutic option in SMZL, which has perioperative and long-term morbidity and mortality, especially in elderly or unfit individuals (Matutes et al., 2008).

The NOTCH pathway, which we show is affected by genetic lesions in up to 30% of SMZLs, may represent an attractive candidate therapeutic target, as some NOTCH inhibitors, such as those preventing its enzymatic conversion to active transcription factor, are already available, and others are under active clinical development (Real et al., 2009). The NF-κB pathway represents an additional potential target; available proteasome inhibitors already approved for other malignancies, or more specific anti–NF-κB compounds currently under development, should be tested for their efficacy in SMZL, either alone or in combination with NOTCH inhibitors.

## MATERIALS AND METHODS

**Patients and tumor biopsies.** The study panel comprised a total of 117 SMZL samples obtained from frozen spleen biopsies of newly diagnosed, previously untreated patients, and was distinguished into a discovery panel ($n = 8$ cases), a screening panel ($n = 32$ cases), and an extension panel ($n = 77$ cases). Out of the 109 SMZLs used as screening and extension panel, 61 were already reported (Rossi et al., 2011). In all cases, the SMZL diagnosis was based on spleen histology and was confirmed by centralized pathological revision (S.A. Pileri). Consistent with a SMZL diagnosis, all cases of the discovery and screening panels lacked the t(11;18) and the t(14;18) translocations (Matutes et al., 2008), and all 117 cases lacked the *BRAF* p.V600E mutation (Swerdlow et al., 2008; Tiacci et al., 2012). Matched normal DNA was obtained from saliva or peripheral blood granulocytes in 48 patients ($n = 8$ discovery cases and 40 cases from the screening and extension panel). The clinical and biological characteristics of cases belonging to the SMZL discovery, screening, and extension panels are summarized in Tables S1, S5, and S6, respectively.

For comparative purposes, 399 B cell tumors other than SMZL were also included in the study (18 nodal MZ lymphomas, 65 extranodal MZ lymphomas, 100 chronic lymphocytic leukemias, 20 mantle cell lymphomas, 20 follicular lymphomas, 134 DLBCLs, 20 *BRAF* p.V600E mutation-positive hairy cell leukemias, and 22 multiple myelomas). All of the 399 samples had been obtained at diagnosis from the involved site (lymph nodes or extranodal sites in the case of lymphoma; $CD138^+$ cells purified from bone marrow aspirates in the case of multiple myeloma; peripheral blood purified B cells in the case of hairy cell leukemia; and peripheral blood mononuclear cells in the case of chronic lymphocytic leukemia). The number of mature

B cell neoplasms included in each panel was estimated to allow a 90% probability of identifying genes that are mutated in at least 10% of cases.

Patients provided informed consent in accordance with local IRB requirements and The Declaration of Helsinki. The study was approved by the Ethical Committee of the Ospedale Maggiore della Carità di Novara affiliated with the Amedeo Avogadro University of Eastern Piedmont (Protocol Code 59/CE; Study Number CE 8/11) and by the Institutional Review Board of Columbia University.

**DNA extraction.** High molecular weight (HMW) genomic DNA was extracted from tumor and normal samples according to standard procedures (Rossi et al., 2011). In all tumor cases, the fraction of tumor cells in the tissue biopsy section used for molecular studies was estimated to be >70% by morphology, immunohistochemistry, and/or flow cytometry. DNA was quantified by the Quant-iT PicoGreen reagent (Invitrogen) in the discovery panel, and by the NanoDrop 2000C spectrophotometer (Thermo Fisher Scientific) in the screening and extension panels. All DNA samples were verified for integrity by 1% agarose gel electrophoresis. Tumor cell clonality was established by amplification of the rearranged *IGH* genes, as described in detail in the paragraph "*IGHV-IGHD-IGHJ* rearrangement analysis." Analysis of patient-specific *IGHV-IGHD-IGHJ* rearrangements were also performed in the paired normal DNA to exclude contamination from tumor cells.

**Whole-exome capture and massively parallel sequencing.** Purified tumor and germline genomic DNA (3 µg) from the 8 discovery SMZL cases was enriched in protein coding sequences using the in-solution exome capture SureSelect Human All Exon 50Mb kit (Agilent Technologies), according to the manufacturer's protocol. The SureSelect Human All Exon 50 Mb kit encompasses all coding exons annotated by the GENCODE project, including all exons in the Consensus CDS (CCDS, March 2009) database, 10 bp of flanking sequence for each targeted region, and small noncoding RNAs from miRBase (v.13) and Rfam. The captured targets were subjected to massively parallel sequencing using the Illumina HiSeq 2000 analyzer (Illumina) with the paired-end 2 × 100 bp read option, following the manufacturer's instructions. As quality controls for the precapture and post-capture steps, randomly selected PCR-amplified clones of the PCR products were subjected to Sanger sequencing to verify their preferential alignment to human genomic regions and to human coding transcripts ($n$ = 50/library). Exome capture and massively parallel sequencing were performed at the HiSeq Service of Fasteris SA (Plan-les-Ouates, Switzerland).

**Sequence mapping and identification of tumor-specific variants.** Paired-end reads (~102.5 million per case) obtained by high-throughput sequencing were aligned to the human genome reference hg19/NCBI GRCh37 using the BWA alignment tool version 0.5.9, and provided a mean depth of 111x with at least 83% of the target exome covered at 30x (Table S2). Sequence variants, i.e., differences from the reference sequence, were identified separately for each tumor and normal sample. The frequency of each variant was estimated from the total number of reads covering the position of that variant. Using the SAVI (Statistical Algorithm for Variant Identification) algorithm developed at Columbia University (Tiacci et al., 2012), an empirical prior was constructed for the variant frequencies. From that prior, we obtained a corresponding high-credibility interval (posterior probability ≥1–$10^{-5}$) for the frequency of each variant and a high-credibility interval for the corresponding change in frequency between the tumor and the normal samples. 218 nonsilent variants, which are not reported in dbSNP 135 and had high posterior probability (≥1–$10^{-5}$) of nonzero presence in the tumor, as well as at least 1% change from the normal with high posterior probability (≥1-$10^{-5}$), were kept for validation by Sanger sequencing. A comparison with data obtained by high-density SNP array analysis of the same tumor/normal pairs established the sensitivity of the method at 96.6% for heterozygous SNP calls and 98% for homozygous SNP calls.

**Validation of candidate somatic mutations by DNA Sanger sequencing.** Candidate nonsilent somatic mutations were subjected to validation by conventional Sanger-based resequencing of PCR products obtained from both tumor and paired normal HMW genomic DNA using primers specific for the exon encompassing the variant. The sequences surrounding the genomic locations of the candidate tumor-specific nonsilent mutations were obtained from the UCSC Human Genome database, and PCR primers were derived from previously published studies (Parsons et al., 2011) or custom-designed using the Primer 3 online software (http://frodo.wi.mit.edu/primer3/). Of the 218 predicted nonsilent variants, 202 (validation rate, 92.6%) were confirmed to be somatic in origin by Sanger sequencing, 6 were also found in the matched normal DNA, thus representing previously nonannotated germline polymorphisms that had not been detected by the high-throughput sequencing analysis, and the remaining 10 variants were absent in both tumor and normal genomic DNA, when tested by Sanger sequencing. Confirmed, somatic nonsynonymous mutations were tested for their functional consequences in silico by using the PolyPhen-2 (Polymorphism Phenotyping) algorithm (http://genetics.bwh.harvard.edu/pph2/), which is based on structure and sequence conservation. Genes found to be mutated were verified for their presence in the Catalogue of Somatic Mutations in Cancer database (Forbes et al., 2011) and in the Cancer Gene Census database.

**Mutation screening of identified genes.** The complete coding sequences and exon–intron junctions of selected genes identified through the whole-exome sequencing and/or the SNP array approach were analyzed in the SMZL screening panel and extension panel by PCR amplification and direct sequencing of whole-genome–amplified DNA obtained using the Repli-g Mini kit (QIAGEN). Sequences for all annotated exons and flanking splice sites were retrieved from the UCSC Human Genome database using the corresponding mRNA accession number as a reference. PCR primers, located ~50 bp upstream or downstream to target exon boundaries, were either derived from previously published studies (Parsons et al., 2011) or designed in the Primer 3 program and filtered using UCSC in silico PCR to exclude pairs yielding more than a single product. All PCR primers and conditions are available upon request. Purified amplicons were subjected to conventional DNA Sanger sequencing using the ABI PRISM 3100 Genetic Analyzer (Applied Biosystems), and compared with the corresponding germline sequences using the Mutation Surveyor Version 3.97 software package (SoftGenetics) after automated and/or manual curation. Of the evaluated sequences, 99% had a Phred score of ≥20 and 96% had a score of ≥30. Candidate somatic mutations were confirmed from both strands on independent PCR products obtained from HMW genomic DNA. Synonymous mutations, previously reported germline polymorphisms, and changes in the matched normal DNA (when available) were removed from the analysis. The following databases were used to exclude known germline variants in primary cases for which paired normal DNA was not available: Human dbSNP Database at NCBI (build 136), Ensembl Database, the 1000 Genomes Project, five single-genome projects available at the UCSC Genome Bioinformatics resource.

**High-density SNP array analysis.** Copy number abnormalities were assessed by high-density SNP array analysis in 81 of the 117 SMZL cases, including the 8 discovery cases (paired tumor and normal DNA), 21 SMZL from the screening panel (both sets using the Genome-Wide Human SNP Array 6.0; Affymetrix), and 52 SMZL cases from the extension panel (using the GeneChip Human Mapping 250K NspI; Affymetrix; GEO accession no. GSE24881). In brief, HMW genomic DNA was restriction enzyme digested, ligated, PCR amplified, purified, labeled, fragmented, and hybridized to the arrays according to the manufacturer's instructions. Identification of segments of abnormal copy numbers were performed using the dChipSNP software, and a karyotype-guided normalization procedure according to a published workflow (Pasqualucci et al., 2011b).

**Whole-transcriptome sequencing (RNA-seq).** Whole-transcriptome sequencing was performed in 6 SMZL cases belonging to the discovery panel (cases 12D through 17D). RNA was extracted from $CD19^+$ B cells

purified from spleen disaggregation using the Allprep DNA/RNA Mini kit (QIAGEN). Polyadenylated RNA was selected after DNaseI treatment and used as a template for double-stranded cDNA synthesis. The 190–210 bp fraction was then isolated and PCR amplified, and libraries were constructed using the Illumina Genome Analyzer paired-end library protocol according to manufacturer's instructions. As quality controls for the precapture and postcapture steps, randomly selected PCR-amplified clones of the PCR products were subjected to Sanger sequencing to verify their preferential alignment to human genomic regions and to human coding transcripts (50 clones/library). Transcriptome sequencing was performed at the HiSeq Service of Fasteris SA (Plan-les-Ouates, Switzerland).

**Whole-transcriptome data analysis.** Reads (mean, 17 M per case) obtained by high-throughput sequencing were aligned to a human transcriptome reference (113 M), obtained by stitching together the exons belonging to the RefSeq transcripts as reported at the UCSC Genome Browser, using the BWA alignment tool version 0.5.9. Sequence variants, i.e., differences from the reference sequence, were identified separately for each sample, and credibility intervals for those frequencies, as well as for the change in frequency from the corresponding whole-exome DNA sequencing, were obtained as described in "Sequence mapping and identification of tumor-specific variants." Expression for each RefSeq transcript was calculated using nonclonal (reads that map to the same exact position are counted once) reads per kilobase of exon model per million mapped reads. For each transcript, we first filter out clonal reads mapping to the same position, and then calculate the mean nonclonal read depth per base and normalize by the total number of nonclonal reads mapped to the transcriptome.

***IGHV-IGHD-IGHJ* rearrangement analysis.** PCR amplification of *IGHV-IGHD-IGHJ* rearrangements was performed on HMW genomic DNA using IGHV leader primers or consensus primers for the IGHV FR1, along with appropriate IGHJ genes, as previously described (Rossi et al., 2011). PCR products were directly sequenced with the ABI PRISM BigDye Terminator v1.1 Ready Reaction Cycle Sequencing kit using the ABI PRISM 3100 Genetic Analyzer (both from Applied Biosystems). Sequences were analyzed using the IMGT databases and the IMGT/V-QUEST tool (version 3.2.17; Centre National de la Recherche Scientifique, LIGM, Université Montpellier 2, Montpellier, France). The following immunogenetic information were recorded for all *IGHV-IGHD-IGHJ* rearrangements: *IGHV* gene and allele usage; percentage of identity to the closest germline *IGHV* allele; VH CDR3 length and composition, including *IGHD*; and *IGHJ* gene usage and *IGHD* gene reading frame. To identify clusters of sequences with common VH CDR3 motifs, sequences were clustered based on the patterns they shared. The VH CDR3 from SMZL was aligned to the VH CDR3 sequences from a database of 28721 samples. Subsets identified as having stereotyped VH CDR3 AA sequences were those characterized by at least 50% amino acid identity and 70% similarity between stereotyped sequences, usage of the same *IGHV* gene, and identical VH CDR3 length (Bikos et al., 2012).

**Fluorescence in situ hybridization (FISH).** In 36 SMZL cases lacking high resolution SNP array data (11 SMZL cases belonging to the screening panel and 25 SMZL cases from the extension panel) the presence of copy number aberrations in selected candidate genes was assessed by FISH analysis, using the following probes: (a) BAC clones RP11-696E2 (*ARID1A*), RP11-177O8 (*BIRC3*), RP11-292B10 (*CREBBP*), RP11-1078O11 (*EP300*), RP11-1113D20 (*GPS2*), RP11-666C2 (*MAP3K14*), RP11-45L15 (*MLL2*), RP11-383D9 (*PTEN*), RP11-622D13 (*SPEN*), RP11-753H20 (*SWAP70*), RP11-122K3 and RP11-996H19 (*TBL1XR1*), RP11-102P5 and RP11-703G8 (*TNFAIP3*), RP11-676M2 (*TRAF3*), RP11-1077G19 (*WAC*); and (b) the commercial probes LSIBCL6 (3q27), LSID7S522-CEP7 (7q31), LSITP53 (17p13.1; Abbott). Labeled BAC probes were tested against normal control metaphases to verify the specificity of the hybridization. For each probe, at least 200 interphase cells with well-delineated fluorescent spots were examined. Nuclei were counterstained with DAPI and antifade reagent, and signals were visualized using a BX51 microscope (Olympus). The presence of copy number abnormalities was scored when the percentage of nuclei showing the abnormality was >10%.

**Immunoblotting.** B cells were purified from the spleen of 3 *NOTCH2* WT and 2 *NOTCH2*-mutated SMZL patients by positive selection, using an anti-CD19 PE antibody, followed by anti-PE microbeads (Miltenyi Biotec). Whole-cell extracts were obtained from CD19-purified SMZL cells or exponentially growing cell lines in RIPA Buffer (140 mM NaCl, 10 mM Tris-HCl, pH 7.5, 0.5% sodium deoxycholate 10x, 0.1% sodium-dodecyl-sulfate + 1% Triton-X 100), according to standard protocols, and proteins were quantified using the Bradford assay. Equivalent amounts of lysates were resolved on 6% SDS-PAGE in reducing conditions. The immunoblot analysis of NOTCH2 expression was performed using a specific anti-NOTCH2 antibody (Bethyl Laboratories) following the manufacturer's instructions. An anti–rabbit HRP-conjugated antibody (Santa Cruz Biotechnology) was used as a secondary reagent. ERK1/2 (BD) was used as loading control. Image acquisition was performed using the ImageQuant LAS4000 software (GE Healthcare).

**RNA extraction and quantitative real-time PCR (qRT-PCR).** RNA was extracted using RNeasy Plus Mini kit (QIAGEN) and converted to cDNA using the High Capacity cDNA Reverse Transcription kit (Applied Biosystems). qRT-PCR was performed using the 7900 HT Fast Real Time PCR System (SDS2.3 software) using commercial primers (TaqMan Gene Expression Assays;Applied Biosystems).The comparative CT method was used to calculate the expression relative to the endogenous control (Serra et al., 2011).

**Statistical analysis.** OS was measured from date of initial presentation to date of death (event) or last follow-up (censoring). PFS was measured from date of initial presentation to date of disease progression or death as a result of any cause, or last follow-up (censoring). Treatment-related mortality was defined as any deaths reported by investigators as probably/possibly related to SMZL treatment. Survival was analyzed by the Kaplan-Meier method and compared by the log-rank test. Categorical variables were compared by $\chi^2$ test and Fisher's exact test when appropriate. Continuous variables were compared by the *t* test. All statistical tests were two-sided. Statistical significance was defined as P value $< 0.05$. The analysis was performed with the Statistical Package for the Social Sciences software v.19.

**Accession codes.** The whole-exome sequencing and copy number data reported in this paper have been deposited in dbGaP under accession no. phs000502.v1.p1 (http://www.ncbi.nlm.nih.gov/projects/gap/cgi-bin/study.cgi?study_id=phs000502.v1.p1).

**Online supplemental material.** Table S1 shows the features of the 8 SMZL discovery cases analyzed by whole-exome sequencing. Table S2 reports the results of Illumina sequencing after whole-exome capture. Table S3 reports the validated somatic mutations identified by whole-exome sequencing in the SMZL discovery panel. Table S4 illustrates the segments (regions) of tumor-acquired copy number alterations identified in the SMZL discovery panel. Table S5 and Table S6 list the patient's features in the screening and extension panel, respectively, Table S7 shows the mutations identified in the screening and extension panels by targeted resequencing of candidate genes. Table S8 reports the copy number aberrations encompassing any of the 61 genes that were subjected to targeted resequencing. Table S9 relates the genetic, immunogenetic and biological features of SMZL and the mutations of MZ development genes. Online supplemental material is available at http://www.jem.org/cgi/content/full/jem.20120904/DC1.

We would like to thank Vladan Miljkovic and the Genomics Technologies Shared Resource of the Herbert Irving Comprehensive Cancer Center at Columbia University for hybridization of the Affymetrix SNP6.0 arrays; Laurent Farinelli and the Fasteris SA facility at Plan-les-Ouates, Geneva, Switzerland, for assistance with the whole-exome capture and sequencing procedure.

This study was supported by AIRC, Special Program Molecular Clinical Oncology, 5 x 1000, No. 10007, Milan, Italy (to G. Gaidano and to R. Foà); Progetto FIRB-Programma "Futuro in Ricerca" 2008 (to D. Rossi and S. Deaglio), PRIN 2008 (to G. Gaidano ), and PRIN 2009 (to D. Rossi), MIUR, Rome, Italy; Progetto Giovani Ricercatori 2008 (to D. Rossi and S. Deaglio) and Ricerca Sanitaria Finalizzata 2008 (to G. Gaidano ), Ministero della Salute, Rome, Italy; Novara-AIL Onlus, Novara, Italy (to G. Gaidano and D. Rossi ); National Institutes of Health grant PO1-CA092625 and a Specialized Center of Research grant from the Leukemia & Lymphoma Society (both to R. Dalla-Favera); Compagnia di San Paolo, Turin, Italy (to R. Foà); Oncosuisse grant OCS-02034-02-2007, Bern, Switzerland (to F. Bertoni); Fondazione Ticinese per la Ricerca sul Cancro, Lugano, Switzerland (to F. Bertoni); SwissLife, Zurich, Switzerland (to F. Bertoni); Nelia and Amedeo Barletta Foundation, Lausanne, Switzerland (to F. Bertoni). S. Monti and S. Cresta are being supported by fellowships from Novara-AIL Onlus, Novara, Italy. S. Rasi is being supported by a fellowship from Società Italiana di Ematologia Sperimentale. G. Fabbri is a Fellow of the American Italian Cancer Foundation.

The authors have no competing financial interests.

**Author contributions**: D. Rossi, R. Dalla-Favera, L. Pasqualucci, and G. Gaidano designed the study, interpreted data, and wrote the manuscript; V.T., J.W. and R.R. developed bioinformatic tools, performed bioinformatic analysis, and contributed to writing the manuscript; M.F. performed and interpreted molecular studies and contributed to writing the manuscript; A.B., S.R., V.S., R.Fa., C.C., M.G., S.C., D.P. and G.F. performed and interpreted mutational analysis; T.V., F.A., V.G. and S.D. performed and interpreted protein expression studies and contributed to writing the manuscript; S.M., C.D. and G.D. performed FISH analysis; A.H., M.M., A.R. and F.B. contributed to analysis of copy number abnormalities; R.S. performed Circos plot analysis; C.A., P.P.P., M.L., F.T., S.F., R.M., F.F., L.A., G.I., S.A.P. and R.Fo. performed diagnosis, provided well characterized pathological samples, and contributed to study design and data interpretation.

**Submitted: 27 April 2012**
**Accepted: 18 July 2012**

## REFERENCES

Bikos, V., N. Darzentas, A. Hadzidimitriou, Z. Davis, S. Hockley, A. Traverse-Glehen, P. Algara, A. Santoro, D. Gonzalez, M. Mollejo, et al. 2012. Over 30% of patients with splenic marginal zone lymphoma express the same immunoglobulin heavy variable gene: ontogenetic implications. *Leukemia*. 26:1638–1646. http://dx.doi.org/10.1038/leu.2012.3

Brennan, A.M., and R.M. Pauli. 2001. Hajdu-Cheney syndrome: evolution of phenotype and clinical problems. *Am. J. Med. Genet.* 100:292–310.

Calado, D.P., B. Zhang, L. Srinivasan, Y. Sasaki, J. Seagal, C. Unitt, S. Rodig, J. Kutok, A. Tarakhovsky, M. Schmidt-Supprian, and K. Rajewsky. 2010. Constitutive canonical NF-κB activation cooperates with disruption of BLIMP1 in the pathogenesis of activated B cell-like diffuse large cell lymphoma. *Cancer Cell*. 18:580–589. http://dx.doi.org/10.1016/j.ccr.2010.11.024

Chopin, M., L. Quemeneur, T. Ripich, and R. Jessberger. 2010a. SWAP-70 controls formation of the splenic marginal zone through regulating T1B-cell differentiation. *Eur. J. Immunol.* 40:3544–3556. http://dx.doi.org/10.1002/eji.201040556

Chopin, M., L. Quemeneur, T. Ripich, and R. Jessberger. 2010b. SWAP-70 controls formation of the splenic marginal zone through regulating T1B-cell differentiation. *Eur. J. Immunol.* 40:3544–3556. http://dx.doi.org/10.1002/eji.201040556

Chopin, M., C.A. Chacón-Martínez, and R. Jessberger. 2011. Fine tuning of IRF-4 expression by SWAP-70 controls the initiation of plasma cell development. *Eur. J. Immunol.* 41:3063–3074. http://dx.doi.org/10.1002/eji.201141742

Chu, Y., J.C. Vahl, D. Kumar, K. Heger, A. Bertossi, E. Wójtowicz, V. Soberon, D. Schenten, B. Mack, M. Reutelshöfer, et al. 2011. B cells lacking the tumor suppressor TNFAIP3/A20 display impaired differentiation and hyperactivation and cause inflammation and autoimmunity in aged mice. *Blood*. 117:2227–2236. http://dx.doi.org/10.1182/blood-2010-09-306019

Conze, D.B., Y. Zhao, and J.D. Ashwell. 2010. Non-canonical NF-κB activation and abnormal B cell accumulation in mice expressing ubiquitin protein ligase-inactive c-IAP2. *PLoS Biol.* 8:e1000518. http://dx.doi.org/10.1371/journal.pbio.1000518

Fabbri, G., S. Rasi, D. Rossi, V. Trifonov, H. Khiabanian, J. Ma, A. Grunn, M. Fangazio, D. Capello, S. Monti, et al. 2011. Analysis of the chronic lymphocytic leukemia coding genome: role of NOTCH1 mutational activation. *J. Exp. Med.* 208:1389–1401. http://dx.doi.org/10.1084/jem.20110921

Forbes, S.A., N. Bindal, S. Bamford, C. Cole, C.Y. Kok, D. Beare, M. Jia, R. Shepherd, K. Leung, A. Menzies, et al. 2011. *Nucleic Acids Res.* 39: D945–D950. http://dx.doi.org/10.1093/nar/gkq929

Gruszka-Westwood, A.M., R.A. Hamoudi, E. Matutes, E. Tuset, and D. Catovsky. 2001. p53 abnormalities in splenic lymphoma with villous lymphocytes. *Blood*. 97:3552–3558. http://dx.doi.org/10.1182/blood.V97.11.3552

Grzenda, A., G. Lomberk, J.S. Zhang, and R. Urrutia. 2009. Sin3: master scaffold and transcriptional corepressor. *Biochim. Biophys. Acta*. 1789: 443–450. http://dx.doi.org/10.1016/j.bbagrm.2009.05.007

Gui, Y., G. Guo, Y. Huang, X. Hu, A. Tang, S. Gao, R. Wu, C. Chen, X. Li, L. Zhou, et al. 2011. Frequent mutations of chromatin remodeling genes in transitional cell carcinoma of the bladder. *Nat. Genet.* 43:875–878. http://dx.doi.org/10.1038/ng.907

Gururajan, M., A. Simmons, T. Dasu, B.T. Spear, C. Calulot, D.A. Robertson, D.L. Wiest, J.G. Monroe, and S. Bondada. 2008. Early growth response genes regulate B cell development, proliferation, and immune response. *J. Immunol.* 181:4590–4602.

Hampel, F., S. Ehrenberg, C. Hojer, A. Draeseke, G. Marschall-Schröter, R. Kühn, B. Mack, O. Gires, C.J. Vahl, M. Schmidt-Supprian, et al. 2011. CD19-independent instruction of murine marginal zone B-cell development by constitutive Notch2 signaling. *Blood*. 118:6321–6331. http://dx.doi.org/10.1182/blood-2010-12-325944

Hermine, O., F. Lefrère, J.P. Bronowicki, X. Mariette, K. Jondeau, V. Eclache-Saudreau, B. Delmas, F. Valensi, P. Cacoub, C. Brechot, et al. 2002. Regression of splenic lymphoma with villous lymphocytes after treatment of hepatitis C virus infection. *N. Engl. J. Med.* 347:89–94. http://dx.doi.org/10.1056/NEJMoa013376

Izon, D.J., J.C. Aster, Y. He, A. Weng, F.G. Karnell, V. Patriub, L. Xu, S. Bakkour, C. Rodriguez, D. Allman, and W.S. Pear. 2002. Deltex1 redirects lymphoid progenitors to the B cell lineage by antagonizing Notch1. *Immunity*. 16:231–243. http://dx.doi.org/10.1016/S1074-7613(02)00271-6

Kridel, R., B. Meissner, S. Rogic, M. Boyle, A. Telenius, B. Woolcock, J. Gunawardana, C. Jenkins, C. Cochrane, S. Ben-Neriah, et al. 2012. Whole transcriptome sequencing reveals recurrent NOTCH1 mutations in mantle cell lymphoma. *Blood*. 119:1963–1971. http://dx.doi.org/10.1182/blood-2011-11-391474

Kuroda, K., H. Han, S. Tani, K. Tanigaki, T. Tun, T. Furukawa, Y. Taniguchi, H. Kurooka, Y. Hamada, S. Toyokuni, and T. Honjo. 2003. Regulation of marginal zone B cell development by MINT, a suppressor of Notch/RBP-J signaling pathway. *Immunity*. 18:301–312. http://dx.doi.org/10.1016/S1074-7613(03)00029-3

Lee, S.Y., K. Kumano, K. Nakazaki, M. Sanada, A. Matsumoto, G. Yamamoto, Y. Nannya, R. Suzuki, S. Ota, Y. Ota, et al. 2009. Gain-of-function mutations and copy number increases of Notch2 in diffuse large B-cell lymphoma. *Cancer Sci.* 100:920–926. http://dx.doi.org/10.1111/j.1349-7006.2009.01130.x

Lenz, G., R.E. Davis, V.N. Ngo, L. Lam, T.C. George, G.W. Wright, S.S. Dave, H. Zhao, W. Xu, A. Rosenwald, et al. 2008. Oncogenic CARD11 mutations in human diffuse large B cell lymphoma. *Science*. 319:1676–1679. http://dx.doi.org/10.1126/science.1153629

Li, J., J. Li, X. Yang, H. Qin, P. Zhou, Y. Liang, and H. Han. 2005. The C terminus of MINT forms homodimers and abrogates MINT-mediated transcriptional repression. *Biochim. Biophys. Acta*. 1729:50–56. http://dx.doi.org/10.1016/j.bbaexp.2005.02.001

Lohr, J.G., P. Stojanov, M.S. Lawrence, D. Auclair, B. Chapuy, C. Sougnez, P. Cruz-Gordillo, B. Knoechel, Y.W. Asmann, S.L. Slager, et al. 2012. Discovery and prioritization of somatic mutations in diffuse large B-cell lymphoma (DLBCL) by whole-exome sequencing. *Proc. Natl. Acad. Sci. USA*. 109:3879–3884. http://dx.doi.org/10.1073/pnas.1121343109

Matsuno, K., M. Ito, K. Hori, F. Miyashita, S. Suzuki, N. Kishi, S. Artavanis-Tsakonas, and H. Okano. 2002. Involvement of a proline-rich motif and RING-H2 finger of Deltex in the regulation of Notch signaling. *Development*. 129:1049–1059.

Matutes, E., D. Oscier, C. Montalban, F. Berger, E. Callet-Bauchu, A. Dogan, P. Felman, V. Franco, E. Iannitto, M. Mollejo, et al. 2008. Splenic marginal zone lymphoma proposals for a revision of diagnostic, staging and therapeutic criteria. *Leukemia*. 22:487–495. http://dx.doi.org/10.1038/sj.leu.2405068

Moran, S.T., A. Cariappa, H. Liu, B. Muir, D. Sgroi, C. Boboila, and S. Pillai. 2007. Synergism between NF-kappa B1/p50 and Notch2 during the development of marginal zone B lymphocytes. *J. Immunol.* 179:195–200.

Morin, R.D., M. Mendez-Lago, A.J. Mungall, R. Goya, K.L. Mungall, R.D. Corbett, N.A. Johnson, T.M. Severson, R. Chiu, M. Field, et al. 2011. Frequent mutation of histone-modifying genes in non-Hodgkin lymphoma. *Nature*. 476:298–303. http://dx.doi.org/10.1038/nature10351

Mullighan, C.G., J. Zhang, L.H. Kasper, S. Lerach, D. Payne-Turner, L.A. Phillips, S.L. Heatley, L. Holmfeldt, J.R. Collins-Underwood, J. Ma, et al. 2011. CREBBP mutations in relapsed acute lymphoblastic leukaemia. *Nature*. 471:235–239. http://dx.doi.org/10.1038/nature09727

Ngo, V.N., R.M. Young, R. Schmitz, S. Jhavar, W. Xiao, K.H. Lim, H. Kohlhammer, W. Xu, Y. Yang, H. Zhao, et al. 2011. Oncogenically active MYD88 mutations in human lymphoma. *Nature*. 470:115–119. http://dx.doi.org/10.1038/nature09671

Oberoi, J., L. Fairall, P.J. Watson, J.C. Yang, Z. Czimmerer, T. Kampmann, B.T. Goult, J.A. Greenwood, J.T. Gooch, B.C. Kallenberger, et al. 2011. Structural basis for the assembly of the SMRT/NCoR core transcriptional repression machinery. *Nat. Struct. Mol. Biol.* 18:177–184. http://dx.doi.org/10.1038/nsmb.1983

Pappu, B.P., and X. Lin. 2006. Potential role of CARMA1 in CD40-induced splenic B cell proliferation and marginal zone B cell maturation. *Eur. J. Immunol.* 36:3033–3043. http://dx.doi.org/10.1002/eji.200535663

Parsons, D.W., M. Li, X. Zhang, S. Jones, R.J. Leary, J.C. Lin, S.M. Boca, H. Carter, J. Samayoa, C. Bettegowda, et al. 2011. The genetic landscape of the childhood cancer medulloblastoma. *Science*. 331:435–439. http://dx.doi.org/10.1126/science.1198056

Pasqualucci, L., D. Dominguez-Sola, A. Chiarenza, G. Fabbri, A. Grunn, V. Trifonov, L.H. Kasper, S. Lerach, H. Tang, J. Ma, et al. 2011a. Inactivating mutations of acetyltransferase genes in B-cell lymphoma. *Nature*. 471:189–195. http://dx.doi.org/10.1038/nature09730

Pasqualucci, L., V. Trifonov, G. Fabbri, J. Ma, D. Rossi, A. Chiarenza, V.A. Wells, A. Grunn, M. Messina, O. Elliot, et al. 2011b. Analysis of the coding genome of diffuse large B-cell lymphoma. *Nat. Genet.* 43:830–837. http://dx.doi.org/10.1038/ng.892

Perissi, V., C. Scafoglio, J. Zhang, K.A. Ohgi, D.W. Rose, C.K. Glass, and M.G. Rosenfeld. 2008. TBL1 and TBLR1 phosphorylation on regulated gene promoters overcomes dual CtBP and NCoR/SMRT transcriptional repression checkpoints. *Mol. Cell.* 29:755–766. http://dx.doi.org/10.1016/j.molcel.2008.01.020

Pillai, S., and A. Cariappa. 2009. The follicular versus marginal zone B lymphocyte cell fate decision. *Nat. Rev. Immunol.* 9:767–777. http://dx.doi.org/10.1038/nri2656

Quesada, V., L. Conde, N. Villamor, G.R. Ordóñez, P. Jares, L. Bassaganyas, A.J. Ramsay, S. Beà, M. Pinyol, A. Martínez-Trillos, et al. 2012. Exome sequencing identifies recurrent mutations of the splicing factor SF3B1 gene in chronic lymphocytic leukemia. *Nat. Genet.* 44:47–52. http://dx.doi.org/10.1038/ng.1032

Real, P.J., V. Tosello, T. Palomero, M. Castillo, E. Hernando, E. de Stanchina, M.L. Sulis, K. Barnes, C. Sawai, I. Homminga, et al. 2009. Gamma-secretase inhibitors reverse glucocorticoid resistance in T cell acute lymphoblastic leukemia. *Nat. Med.* 15:50–58. http://dx.doi.org/10.1038/nm.1900

Rinaldi, A., M. Mian, E. Chigrinova, L. Arcaini, G. Bhagat, U. Novak, P.M. Rancoita, C.P. De Campos, F. Forconi, R.D. Gascoyne, et al. 2011. Genome-wide DNA profiling of marginal zone lymphomas identifies subtype-specific lesions with an impact on the clinical outcome. *Blood*. 117:1595–1604. http://dx.doi.org/10.1182/blood-2010-01-264275

Robledo, C., J.L. García, R. Benito, T. Flores, M. Mollejo, J.A. Martínez-Climent, E. García, N.C. Gutiérrez, M.A. Piris, and J.M. Hernández. 2011. Molecular characterization of the region 7q22.1 in splenic marginal zone lymphomas. *PLoS ONE*. 6:e24939. http://dx.doi.org/10.1371/journal.pone.0024939

Rossi, D., S. Deaglio, D. Dominguez-Sola, S. Rasi, T. Vaisitti, C. Agostinelli, V. Spina, A. Bruscaggin, S. Monti, M. Cerri, et al. 2011. Alteration of BIRC3 and multiple other NF-κB pathway genes in splenic marginal zone lymphoma. *Blood*. 118:4930–4934. http://dx.doi.org/10.1182/blood-2011-06-359166

Rossi, D., S. Rasi, G. Fabbri, V. Spina, M. Fangazio, F. Forconi, R. Marasca, L. Laurenti, A. Bruscaggin, M. Cerri, et al. 2012. Mutations of NOTCH1 are an independent predictor of survival in chronic lymphocytic leukemia. *Blood*. 119:521–529. http://dx.doi.org/10.1182/blood-2011-09-379966

Saito, T., S. Chiba, M. Ichikawa, A. Kunisato, T. Asai, K. Shimizu, T. Yamaguchi, G. Yamamoto, S. Seo, K. Kumano, et al. 2003. Notch2 is preferentially expressed in mature B cells and indispensable for marginal zone B lineage development. *Immunity*. 18:675–685. http://dx.doi.org/10.1016/S1074-7613(03)00111-0

Salido, M., C. Baró, D. Oscier, K. Stamatopoulos, J. Dierlamm, E. Matutes, A. Traverse-Glehen, F. Berger, P. Felman, C. Thieblemont, et al. 2010. Cytogenetic aberrations and their prognostic value in a series of 330 splenic marginal zone B-cell lymphomas: a multicenter study of the Splenic B-Cell Lymphoma Group. *Blood*. 116:1479–1488. http://dx.doi.org/10.1182/blood-2010-02-267476

Santos, M.A., L.M. Sarmento, M. Rebelo, A.A. Doce, I. Maillard, A. Dumortier, H. Neves, F. Radtke, W.S. Pear, L. Parreira, and J. Demengeot. 2007. Notch1 engagement by Delta-like-1 promotes differentiation of B lymphocytes to antibody-secreting cells. *Proc. Natl. Acad. Sci. USA*. 104:15454–15459. http://dx.doi.org/10.1073/pnas.0702891104

Sasaki, Y., D.P. Calado, E. Derudder, B. Zhang, Y. Shimizu, F. Mackay, S. Nishikawa, K. Rajewsky, and M. Schmidt-Supprian. 2008. NIK overexpression amplifies, whereas ablation of its TRAF3-binding domain replaces BAFF:BAFF-R-mediated survival signals in B cells. *Proc. Natl. Acad. Sci. USA*. 105:10883–10888. http://dx.doi.org/10.1073/pnas.0805186105

Serra, S., A.L. Horenstein, T. Vaisitti, D. Brusa, D. Rossi, L. Laurenti, G. D'Arena, M. Coscia, C. Tripodo, G. Inghirami, S.C. Robson, G. Gaidano, F. Malavasi, and S. Deaglio. 2011. CD73-generated extracellular adenosine in chronic lymphocytic leukemia creates local conditions counteracting drug-induced cell death. *Blood*. 118:6141–6152.

Simpson, M.A., M.D. Irving, E. Asilmaz, M.J. Gray, D. Dafou, F.V. Elmslie, S. Mansour, S.E. Holder, C.E. Brain, B.K. Burton, et al. 2011. Mutations in NOTCH2 cause Hajdu-Cheney syndrome, a disorder of severe and progressive bone loss. *Nat. Genet.* 43:303–305. http://dx.doi.org/10.1038/ng.779

Suarez, F., O. Lortholary, O. Hermine, and M. Lecuit. 2006. Infection-associated lymphomas derived from marginal zone B cells: a model of antigen-driven lymphoproliferation. *Blood*. 107:3034–3044. http://dx.doi.org/10.1182/blood-2005-09-3679

Swerdlow, S.H. E. Campo, N.L. Harris, E.S. Jaffe, S.A. Pileri, H. Stein, J. Thiele, and J.W. Vardiman. 2008. WHO classification of tumours of haematopoietic and lymphoid tissues, Fourth Edition. Lyon, France.

Tiacci, E., G. Schiavoni, F. Forconi, A. Santi, L. Trentin, A. Ambrosetti, D. Cecchini, E. Sozzi, P. Francia di Celle, C. Di Bello, et al. 2012. Simple genetic diagnosis of hairy cell leukemia by sensitive detection of the BRAF-V600E mutation. *Blood*. 119:192–195. http://dx.doi.org/10.1182/blood-2011-08-371179

Traverse-Glehen, A., L. Baseggio, G. Salles, P. Felman, and F. Berger. 2011. Splenic marginal zone B-cell lymphoma: a distinct clinicopathological and molecular entity. Recent advances in ontogeny and classification. *Curr. Opin. Oncol.* 23:441–448. http://dx.doi.org/10.1097/CCO.0b013e328349ab8d

Trøen, G., I. Wlodarska, A. Warsame, S. Hernández Llodrà, C. De Wolf-Peeters, and J. Delabie. 2008. NOTCH2 mutations in marginal zone lymphoma. *Haematologica*. 93:1107–1109.

VanderWielen, B.D., Z. Yuan, D.R. Friedmann, and R.A. Kovall. 2011. Transcriptional repression in the Notch pathway: thermodynamic characterization of CSL-MINT (Msx2-interacting nuclear target protein) complexes. *J. Biol. Chem.* 286:14892–14902. http://dx.doi.org/10.1074/jbc.M110.181156

Wang, L., M.S. Lawrence, Y. Wan, P. Stojanov, C. Sougnez, K. Stevenson, L. Werner, A. Sivachenko, D.S. DeLuca, L. Zhang, et al. 2011a. SF3B1 and other novel cancer genes in chronic lymphocytic leukemia. *N. Engl. J. Med.* 365:2497–2506. http://dx.doi.org/10.1056/NEJMoa1109016

Wang, N.J., Z. Sanborn, K.L. Arnett, L.J. Bayston, W. Liao, C.M. Proby, I.M. Leigh, E.A. Collisson, P.B. Gordon, L. Jakkula, et al. 2011b. Loss-of-function mutations in Notch receptors in cutaneous and lung squamous cell carcinoma. *Proc. Natl. Acad. Sci. USA.* 108:17761–17766. http://dx.doi.org/10.1073/pnas.1114669108

Warsame, A.A., H.C. Aasheim, K. Nustad, G. Trøen, A. Tierens, V. Wang, U. Randen, H.P. Dong, S. Heim, A. Brech, and J. Delabie. 2011. Splenic marginal zone lymphoma with VH1-02 gene rearrangement expresses poly- and self-reactive antibodies with similar reactivity. *Blood.* 118:3331–3339. http://dx.doi.org/10.1182/blood-2011-03-341651

Watkins, A.J., Y. Huang, H. Ye, E. Chanudet, N. Johnson, R. Hamoudi, H. Liu, G. Dong, A. Attygalle, E.D. McPhail, et al. 2010. Splenic marginal zone lymphoma: characterization of 7q deletion and its value in diagnosis. *J. Pathol.* 220:461–474.

Weng, A.P., A.A. Ferrando, W. Lee, J.P. Morris IV, L.B. Silverman, C. Sanchez-Irizarry, S.C. Blacklow, A.T. Look, and J.C. Aster. 2004. Activating mutations of NOTCH1 in human T cell acute lymphoblastic leukemia. *Science.* 306:269–271. http://dx.doi.org/10.1126/science.1102160

Wiegand, K.C., S.P. Shah, O.M. Al-Agha, Y. Zhao, K. Tse, T. Zeng, J. Senz, M.K. McConechy, M.S. Anglesio, S.E. Kalloger, et al. 2010. ARID1A mutations in endometriosis-associated ovarian carcinomas. *N. Engl. J. Med.* 363:1532–1543. http://dx.doi.org/10.1056/NEJMoa1008433

Xie, P., L.L. Stunz, K.D. Larison, B. Yang, and G.A. Bishop. 2007. Tumor necrosis factor receptor-associated factor 3 is a critical regulator of B cell homeostasis in secondary lymphoid organs. *Immunity.* 27:253–267. http://dx.doi.org/10.1016/j.immuni.2007.07.012

Yan, Q., Y. Huang, A.J. Watkins, S. Kocialkowski, N. Zeng, R.A. Hamoudi, P.G. Isaacson, L. de Leval, A. Wotherspoon, and M.Q. Du. 2012. BCR and TLR signaling pathways are recurrently targeted by genetic changes in splenic marginal zone lymphomas. *Haematologica.* 97:595–598. http://dx.doi.org/10.3324/haematol.2011.054080

Yuan, J.S., P.C. Kousis, S. Suliman, I. Visan, and C.J. Guidos. 2010. Functions of notch signaling in the immune system: consensus and controversies. *Annu. Rev. Immunol.* 28:343–365. http://dx.doi.org/10.1146/annurev.immunol.021908.132719

Zweifel, M.E., D.J. Leahy, and D. Barrick. 2005. Structure and Notch receptor binding of the tandem WWE domain of Deltex. *Structure.* 13:1599–1611. http://dx.doi.org/10.1016/j.str.2005.07.015

SUPPLEMENTAL MATERIAL

Rossi et al., http://www.jem.org/cgi/content/full/jem.20120904/DC1

**Table S1, which is presented as an Excel file, shows the features of the 8 SMZL discovery cases analyzed by whole-exome sequencing.**

**Table S2, which is presented as an Excel file, reports the results of Illumina sequencing after whole-exome capture.**

**Table S3, which is presented as an Excel file, reports the validated somatic mutations identified by whole-exome sequencing in the SMZL discovery panel.**

**Table S4, which is presented as an Excel file, illustrates the segments (regions) of tumor-acquired copy number alterations identified in the SMZL discovery panel.**

**Table S5, which is presented as an Excel file, and Table S6 list the patient's features in the screening and extension panel, respectively.**

**Table S7, which is presented as an Excel file, shows the mutations identified in the screening and extension panels by targeted resequencing of candidate genes.**

**Table S8, which is presented as an Excel file, reports the copy number aberrations encompassing any of the 61 genes that were subjected to targeted resequencing.**

**Table S9, which is presented as an Excel file, relates the genetic, immunogenetic, and biological features of SMZL and the mutations of MZ development genes.**